Magnetoplasmons in an electron gas at the crossover from two- to one-dimensional behavior

U. Wulf
Max-Planck-Institut für Festkörperforschung, Heisenbergstrasse 1, D-7000 Stuttgart 80, Federal Republic of Germany

E. Zeeb and P. Gies
Physikalisches Institut der Universität Würzburg, Am Hubland, D-8700 Würzburg, Federal Republic of Germany

R. R. Gerhardts
Max-Planck-Institut für Festkörperforschung, Heisenbergstrasse 1, D-7000 Stuttgart 80, Federal Republic of Germany

W. Hanke
Physikalisches Institut der Universität Würzburg, Am Hubland, D-8700 Würzburg, Federal Republic of Germany

(Received 3 July 1990)

Magnetoplasmons in a strongly modulated two-dimensional electron gas are studied within the random-phase approximation, including for the first time local fields as well as screening effects in the ground state. With increasing modulation a transition from "bulk" to "edge" magnetoplasmons accompanied by a frequency lowering is observed. Our results open a new interpretation of recent far-infrared experiments and correct predictions of classical model calculations that become unphysical for submicrometer systems.

With modern microstructuring techniques the quasi-two-dimensional electron gas (2D EG) in, e.g., a GaAs/(Al,Ga)As heterostructure can be laterally confined on a submicrometer scale to quasi-one-dimensional (1D) structures (quantum wires) or quasi-zero-dimensional dots.[1-5] Size quantization of electronic energy levels due to the lateral confinement has clearly been demonstrated by magnetotransport measurements on quantum wires with a width less than 500 nm.[3,4] In view of the great importance of optical methods such as far-infrared (FIR) spectroscopy, the interesting question arises how the size quantization affects the spectra. Although some recent FIR data have been interpreted in terms of transitions between single-particle levels,[2,5] it has been emphasized that in general the FIR radiation excites collective oscillations in many-electron systems.[4,6] In order to interpret FIR experiments correctly, it is, therefore, important to understand the nature of plasmons and magnetoplasmons in these geometrically confined, submicrometer electron systems.

So far, the FIR experiments have usually been evaluated on the basis of the well-known dispersion relation for magnetoplasmons in an unmodulated 2D EG,

$$\omega^2=\omega_c^2+2\pi e^2 n_s q/m\kappa\ , \tag{1}$$

where ω and q are the frequency and (in-plane) wave number of the plasmon, ω_c is the cyclotron frequency, m and κ are the effective mass and dielectric constant, and n_s is the areal density of the 2D EG. For example, Hansen *et al.*,[2] who have studied the transition from a weakly modulated 2D EG to a quantum-wire superlattice by applying a depletion voltage V_g between the 2D EG and a microstructured grating gate, observed (for small modulation) a linear decrease of the squared resonance frequency with V_g and used Eq. (1) to calculate an average density $\bar{n}_s$ of the modulated 2D EG, assuming $q=2\pi/a$, with a the period of the grating gate. Demel *et al.*[4] determined a width W of their quantum wires from Eq. (1). For a plasma wave having nodes on opposite edges of the wires, $q=\pi/W$ ("plasmon in a box"), they obtained much larger W values than from their transport measurements. They argued that modified boundary conditions might resolve this discrepancy.[4]

We demonstrate in this Brief Report that the interpretation of FIR experiments on such submicrometer systems on the basis of Eq. (1) in general is not justified and ignores important physics. We present magnetoplasmon results obtained from a fully quantum-mechanical calculation within the random-phase approximation (RPA), based on a model of a 2D EG in a sinusoidal modulation potential of arbitrary strength, which covers the whole region between 2D and 1D behavior. We, thus, are able to compare our results with the experiments of Ref. 2 in this most interesting transition region. This was neither possible in previous RPA calculations, which were restricted to zero magnetic field and nonoverlapping wires,[7] nor in a recent Letter,[8] presenting magnetoplasmon results for the case of weak modulation and the limit of very low frequencies. Furthermore, we fully include the "local-field effects" (due to higher-reciprocal-lattice vectors) on the response in the periodically modulated ground state, which were neglected in Ref. 8. Thus, we are able to investigate the detailed shape of plasma oscillations, which was previously discussed only in a classical local-response approximation (LRA).[9,10]

Our results show, similar to the LRA, that with increasing density modulation $n_s(x)$ the plasma oscillation

is expelled from the high-density regions, so that the amplitude of the oscillation becomes largest where $n_s(x)$ is small, and the frequency decreases. Our quantum theory corrects, however, the unphysical prediction of the LRA that both width and frequency of the plasma oscillation approach zero as the minima of $n_s(x)$ approach zero. This prediction was in clear contradiction to the experiments of Hansen *et al.*,[2] which yield at the transition from the modulated 2D EG to nonoverlapping 1D wires a plasmon excitation with a finite frequency of the same order of magnitude as for the unmodulated system. Hansen *et al.* used the reduction of the plasmon frequency observed during this transition to calculate from Eq. (1) an average electron density ($\bar{n}_s = 1.8\times10^{11}$ cm^{-2} at the channel formation, $\bar{n}_s = 6\times10^{11}$ cm^{-2} at zero gate voltage). Thus, it was assumed that the depletion of electrons from the 2D EG, caused by the applied gate voltage that creates the modulation, is the only reason for the observed frequency lowering. However, our results reveal a frequency-lowering mechanism inherently related to the increase of the density modulation in the ground state at constant average electron density $\bar{n}_s$, which also explains why the simple plasmon-in-a-box model leads to problems with the wire width.[4] In order to separate clearly the frequency lowering due to the increase of the modulation from the lowering due to the decrease of the average electron density $\bar{n}_s$, we study different strengths of the modulation while keeping $\bar{n}_s$ fixed, which, unfortunately, was not possible in the experiment.[2]

As a model system we consider a GaAs-(Al,Ga)As heterostructure ($m = 0.07m_0$; $\kappa = 11.9$; $n_s = 2\times10^{11}$ cm^{-2}) with a laterally microstructured gate electrode of period $a = 500$ nm in the x direction, as described in Ref. 2. The effect of the microstructured gate can well be simulated by an external potential (created by the gate charges) of the form $V_0 + V_m\cos[(2\pi/a)x]$ in the gate surface at a distance $D = 26$ nm from the GaAs-(Al,Ga)As interface.[11] The 2D EG is strictly confined to the lowest electrical subband.

The plasmon eigenmodes of the system can be obtained, within the RPA, as the zeros of the determinant of the dielectric-response matrix $\epsilon_{GG'}$, which is conveniently expressed, in the Fourier representation, as[12]

$$\epsilon_{GG'}(q_x,q_y;\omega) = \delta_{GG'} - v(q_x+G,q_y;\omega) \times P^0(q_x+G,q_x+G',q_y;\omega) \ . \quad (2)$$

Here, $G = m(2\pi/a)$, $m = 0,\pm1,\pm2,\ldots$, is the 1D reciprocal-lattice vector in the x direction, q_x the corresponding momentum in the first Brillouin zone, [i.e., $-(\pi/a) < q_x \le (\pi/a)$], and q_y is the momentum in the y direction along the channels. As usual P^0 denotes the irreducible polarization matrix, here calculated from a self-consistently determined effective potential including the magnetic-field-dependent screening effects in the Hartree approximation[11] and v is the Coulomb interaction. For an explicit representation as well as for computational details we refer to Ref. 12. The calculations are performed for $q_y = 0$, i.e., we assume electron gas as well as exciting electromagnetic field constant in the y direction. As can be shown easily, the RPA plasmon frequency in the *homogeneous* 2D EG is, up to first order in the momentum q, given by Eq. (1). In the range of larger q the RPA dispersion shows a maximum and falls off exponentially to ω_c for q going to infinity. This is an artifact of the RPA and is corrected by exchange-correlation effects.[13] In order to avoid such problems we include in our RPA calculation *for the structured system* only values of $q = |q_x + G|$ up to the dispersion maximum, thus restricting the rank of the matrix $\epsilon_{GG'}$ to, e.g., 21 at $B = 10$ T and 5 at $B = 2$ T.

The characteristic changes of the magnetoplasmon frequency at the transition from 2D to 1D behavior can be seen in Fig. 1, showing, for $B = 10$ T, the four lowest eigenfrequencies in the center of the first 1D Brillouin zone (BZ), $q_x = 0$,[14] versus the amplitude $-V_m$ of the modulation potential. (The sign is adapted to the experimental situation.) The four modes ($N = 1,\ldots,4$) considered here, evolve with increasing modulation (larger $-V_m$) from the magnetoplasmons of the homogeneous system ($V_m = 0$) with $q_x = 0$ ($N = 1$), $\pm2\pi/a$ ($N = 2,3$), and $\pm4\pi/a$ ($N = 4$, mode 5 not shown) after backfolding into the first BZ. These $q_x = 0$ modes can in principle be excited by FIR light ($|q_x| \ll 2\pi/a$) with the gate acting as a grating coupler or, with the same result, the modulation of the electron density breaking the translational invariance. The hatched area labels the particle-hole excitations.[15] In the unmodulated 2D system the $N = 1$ mode coincides with the cyclotron resonance and the higher modes are given by Eq. (1). With increasing modulation (larger $-V_m$), the lowest mode increases very slightly in energy, whereas the higher modes decrease strongly up to a modulation potential of $V_m \approx -90$ meV, even though the mean density is fixed. From the ground-state calculation, we can identify this as the threshold voltage where the 2D EG splits into 1D channels, that is, where the electronic density between the channels is about one hundred times smaller than in the center of a channel.

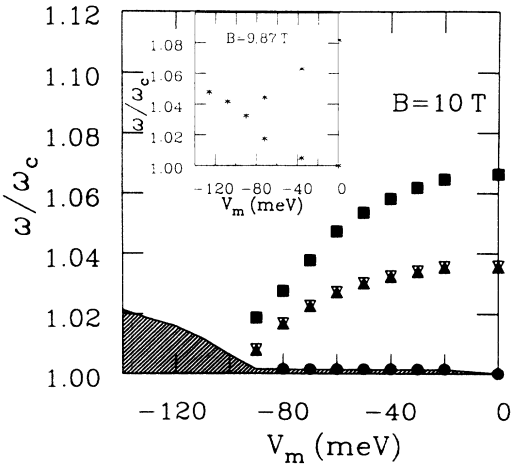

FIG. 1. The four lowest magnetoplasmon modes at $q_x = 0$ with $B = 10$ T and $q_y = 0$. For $N = 1$ (notation see text) we used solid circles, for $N = 2$ solid triangles, $N = 3$ open triangles, and $N = 4$ solid squares. The hatched area marks the particle-hole continuum. The inset shows the experimental data of Ref. 16. The gate voltage is rescaled by a constant factor, so that the threshold occurs at -90 meV.

Beyond this threshold voltage ($V_m < -90$ meV), the plasmon frequencies fall into the spectrum of single-particle excitations. We understand the single-particle spectrum from the ground-state calculations. In the quasi-1D situation the Landau bands near the Fermi level fail to be parallel, and a single-particle continuum opens, whereas in the quasi-2D situation of weaker modulation the nearly perfect screening leads to nearly parallel Landau bands,[11] and thus to a very narrow excitation spectrum for $q_x = q_y = 0$. Below we will give an argument based on a parabolic approximation of the external potential that shows the optically active collective mode in the 1D region ($V_m < 90$ meV) is essentially a rigid center-of-mass motion, which is decoupled from the internal degrees of freedom and, therefore, undamped although its frequency in the present case, $B = 10$ T, falls into the single-particle continuum. The inset in Fig. 1 shows the corresponding experimental result[16] at $B = 9.87$ T. The two modes in the measurement can be identified as evolving from the magnetoplasmon resonances of the unmodulated system at $q_x = 0$ (cyclotron resonance; $N = 1$ mode) and $q_x = \pm 2/a$ (plasmonic mode, will be called *umklapp* resonance in this paper; $N = 2, 3$), respectively. Note that the total decrease of frequency experimentally observed for this *umklapp* resonance is only about twice the value we calculated for fixed average density, $\bar{n}_s = 2 \times 10^{11}$ cm^{-2}. This demonstrates that in the experiment the frequency lowering due to the increase of the modulation must be a very important effect. As a consequence, the actual mean density at the transition ($V_m = -90$ meV) is larger than estimated from Eq. (1). For $V_m < -90$ meV, where only particle-hole excitations are seen in the calculation, the experiment shows a quite broad single resonance, located near the upper edge of particle-hole continuum.

Figure 2 shows the magnetoplasmon resonances, for the system studied above, at $B = 2$ T. Here, the transition from 2D to 1D behavior still occurs at $V_m = -90$ meV, but the *umklapp* resonances clearly remain above the single-particle spectrum; they do not become Landau damped. The upper resonance even increases slightly in energy, as the voltage gets smaller than $V_m = -90$ meV, similar, but less pronounced as in the experiment, which is also shown in Fig. 2. The lowest excitation ($N = 1$) lies now inside the particle-hole continuum which, owing to the less-effective screening,[11] now appears broader than for $B = 10$ T. The quantitative differences between experiment and theory can be attributed, first of all, to the variation of the electron density with the gate voltage, which we have not taken into account, and second, to the simple form of the external potential we assumed in the calculation. Replacing $V_m \cos[(2\pi/a)x]$ by the steeper potential $V_m \cos(2\pi\{(x/a) - \frac{6}{100}\sin[(2\pi/a)x]\})$, which is more adequate for the actual gate structure,[2,16] we observed that the gap between the two *umklapp* modes becomes larger and the upper resonance is shifted further upwards (solid circles in Fig. 2) leading to a closer agreement with the experiment.

The character of the magnetoplasmon resonances is most clearly visible in the induced density profile $\delta\rho(x)$.

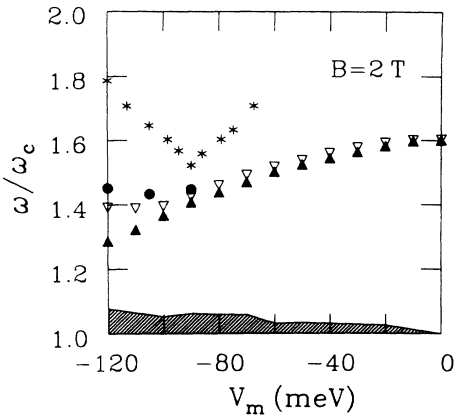

FIG. 2. The $N = 2$ (solid triangle) and $N = 3$ (open triangle) magnetoplasmon mode at $q = 0$ with $B = 2$ T and $q_y = 0$. The hatched area marks the particle-hole continuum. The (rescaled) experimental results of Ref. 16 for $B = 2.19$ T are shown by the asterisks, those for the steeper potential (text) by solid circles.

Results for the third ($N = 3$) magnetoplasmon excitation corresponding to the open triangles in Fig. 1 at $V_m = -50$ meV and at $V_m = -90$ meV are shown in Fig. 3. At $V_m = -50$ meV, the real and imaginary parts of the plasma wave, which are cosine-like and sine-like, respectively, in the unmodulated 2D EG, are deformed towards the edges of the channel. Mathematically, this deformation is due to local-field effects arising from higher-reciprocal-lattice vectors G, cf. Eq. (2). By increasing the voltage towards the threshold value of 1D-channel formation, the *induced* density becomes small in the center of the channel and localized at the edges [Fig. 3(b)]. In addition, the symmetric (real) part of the oscillations vanishes (the small oscillations in the density profile are a numerical artifact due to our truncation of $\epsilon_{GG'}$ to a finite-rank matrix). The second model (solid triangles in Figs. 1 and 2, $N = 2$) turns out to be of similar shape but with a predominant symmetric component. The larger dipole moment of the antisymmetric (third) mode and its increasing frequency with increasing $-V_m$ beyond 90 meV show that this mode is the optical active one. These results resemble the findings of the classical local-response model,[10,9] although in our quantum-mechanical model, the localization of the plasma oscillations is less pronounced, especially as the magnetic field becomes smaller [see Fig. 3(c)].

In the quasi-1D limit of strong modulation ($-V_m \geq 90$ meV) we can compare our results for the antisymmetric (third) mode to a rigid oscillation of all electrons in a single quantum wire with a parabolic confinement potential $V_c = \frac{1}{2} m \Omega^2 x^2$. Here the center-of-mass motion decouples exactly from the relative motion since the corresponding Hamiltonians are strictly additive, irrespective of the Coulomb interaction. In the dipole approximation (valid for $q_y = 0$ and $|q_x| \ll 2\pi/a$) the FIR light excites only the centers-of-mass oscillation at frequency $\omega = (\omega_c^2 + \Omega^2)^{1/2}$ as has been shown recently by Brey *et al.*[17] using more formal arguments. (A corresponding theorem holds for quantum dots and explains recent experiments.[5,6]) If we approximate our external modulation potential propor-

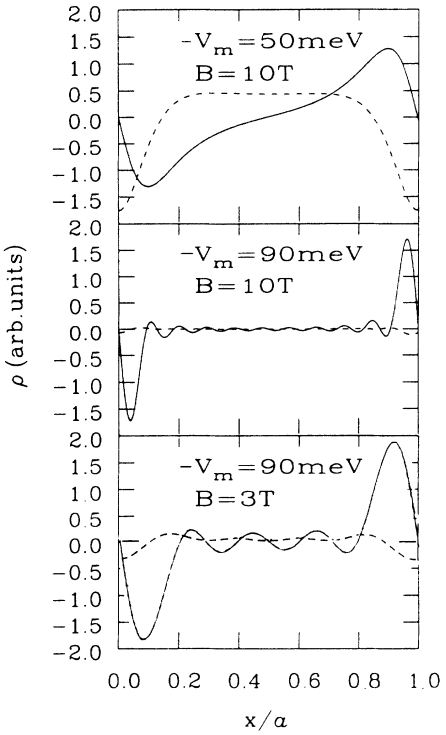

FIG. 3. Magnetoplasmon profiles (Ref. 14) for the $N=3$ mode (corresponding to the open triangles in Fig. 1), vs position x. Solid and dashed lines correspond to, respectively, the imaginary part and the real part of the induced density.

tional to $V_m \exp[-(D+z)(2\pi/a)]\cos[x(2\pi/a)]$ in the plane $z=10$ nm (center of the plane of the 2D EG) by a parabolic potential, we obtain, for $V_m=-90$ meV, $\hbar\Omega \approx 3.2$ meV. This yields $\omega/\omega_c=1.02$ for $B=10$ T and $\omega/\omega_c=1.36$ for $B=2$ T and a corresponding increase of ω/ω_c with increasing values of $-V_m$ or with a steeper potential shape at the gate as shown in Fig. 2 (solid circles). Considering the frequencies and the antisymmetric shape of the induced charge-density profile, we thus may interpret the $N=3$ mode in the 1D limit ($-V_m \geq 90$ meV) as an approximately rigid in-phase oscillation of all the wires. (The corresponding antiphase oscillation has $q_x \approx \pi/a$.) Near the threshold of channel formation ($V_m \approx -90$ meV) the calculated $\delta\rho$ profiles are localized closer to the edges of the channels than one would expect from a rigid oscillation of the ground-state density profile. We attribute this to the deviation of the external cosine potential from the parabolic approximation. Within the crude parabolic approximation we can also understand qualitatively the symmetric ($N=2$) mode as an oscillation of the width of the individual density profile without a center-of-mass motion. This mode should have a lower frequency and is not excited in the dipole approximation.

In summary, we have presented a quantum theory of magnetoplasmons in a density modulated 2D EG, which covers the whole region between 2D behavior and weakly coupled 1D wires. We found that, with increasing modulation, the character of the plasmons changes from a 2D "bulk plasmon" towards a kind of "edge plasmon," and that the plasmon frequency decreases below the value one would obtain from the "bulk" formula Eq. (1) with the average electron density $\bar{n}_s$. Our results open a new interpretation and better understanding of the FIR experiments[2,4,16] on microstructured (Al,Ga)As systems.

We have recently received work by Dahl[18] which presents interesting results on oscillator strengths of plasmons in density-modulated electron systems focusing also on the transition between 2D and 1D behavior, but only for zero magnetic field.

We gratefully acknowledge many informative discussions with D. Heitmann and T. Demel. The work was supported by the Bundesministerium für Forschung und Technologie, West Germany (Grant No. NT-2718-C).

[1] *Physics and Technology of Submicron Structures*, Vol. 38 of *Springer Series in Solid-State Science* edited by H. Heinrich, G. Bauer, and F. Kuchar (Springer-Verlag, Berlin, 1988).

[2] W. Hansen, M. Horst, J. P. Kotthaus, U. Merkt, Ch. Sikorski, and K. Ploog, Phys. Rev. Lett. **58**, 2586 (1987).

[3] K.-F. Berggren, T. J. Thornton, D. J. Newson, and M. Pepper, Phys. Rev. Lett. **57**, 1769 (1986).

[4] T. Demel, D. Heitmann, P. Grambow, and K. Ploog, Phys. Rev. B **38**, 12 732 (1988).

[5] Ch. Sikorski and U. Merkt, Phys. Rev. Lett. **62**, 2164 (1989).

[6] The data of Ref. 5 can also be explained by a rigid motion of the electrons in a dot, since the FIR radiation excites only the center-of-mass motion which, in the assumed parabolic confinement potential, separates from the relative motion and leads to exactly the single-particle energy and excitation spectrum.

[7] W. M. Que and G. Kirczenow, Phys. Rev. B **39**, 5998 (1989); Q. Li and S. Das Sarma, *ibid.* **40**, 5860 (1989).

[8] H. L. Cui, V. Fessatidis, and N. J. M. Horing, Phys. Rev. Lett. **63**, 2598 (1989).

[9] V. Cataudella and V. M. Ramaglia, Phys. Rev. B **38**, 1828 (1988).

[10] G. Eliasson, P. Hawrylak, J.-W. Wu, and J. J. Quinn, Solid State Commun. **60**, 3 (1986).

[11] U. Wulf, Phys. Rev. B **35**, 9754 (1987); U. Wulf and R. R. Gerhardts, *Physics and Technology of Submicron Structures* (Ref. 1), p. 162.

[12] U. Wulf, E. Zeeb, P. Gies, R. R. Gerhardts, and W. Hanke, Phys. Rev. B **41**, 3113 (1990).

[13] C. Kallin and B. I. Halperin, Phys. Rev. B **30**, 5655 (1984).

[14] For reasons of numerical stability, the excitations at zero wave vector are calculated for small but finite $q_x=10^3$ cm^{-1}.

[15] Only particle-hole excitations with an occupation number difference, according to the Fermi distribution at a temperature of $T=1$ K, of more than 10^{-2} are displayed in the figure.

[16] W. Hansen and J. P. Kotthaus, *Physics and Technology of Submicron Structures* (Ref. 1), p. 187.

[17] L. Brey, N. F. Johnson, and B. I. Halperin, Phys. Rev. B **40**, 10 647 (1989).

[18] C. Dahl, Phys. Rev. B **41**, 5763 (1990).